THE JOURNAL OF BIOLOGICAL CHEMISTRY VOL. 291, NO. 49, pp. 25678–25691, December 2, 2016

Regulation of TRPP3 Channel Function by N-terminal Domain Palmitoylation and Phosphorylation*

Received for publication, August 31, 2016, and in revised form, October 16, 2016 Published, JBC Papers in Press, October 17, 2016, DOI 10.1074/jbc.M116.756544

Wang Zheng[‡1], JungWoo Yang[‡], Erwan Beauchamp[§], Ruiqi Cai[‡], Shaimaa Hussein[‡], Laura Hofmann[¶], Qiang Li[‡], Veit Flockerzi[¶], Luc G. Berthiaume[§], Jingfeng Tang[‖2], and Xing-Zhen Chen[‡‖3]

From the Membrane Protein Disease Research Group, [‡]Departments of Physiology and [§]Cell Biology, Faculty of Medicine and Dentistry, University of Alberta, Edmonton, Alberta T6G 2H7, Canada, the [¶]Experimentelle und Klinische Pharmakologie und Toxikologie, Universität des Saarlandes, 66421 Homburg, Germany, and the [‖]Institute of Biomedical and Pharmaceutical Sciences and Provincial Cooperative Innovation Center, College of Bioengineering, Hubei University of Technology, 430068 Wuhan, China

Edited by Roger Colbran

Transient receptor potential polycystin-3 (TRPP3) is a cation channel activated by calcium and proton and is involved in hedgehog signaling, intestinal development, and sour tasting. How TRPP3 channel function is regulated remains poorly understood. By N-terminal truncation mutations, electrophysiology, and *Xenopus* oocyte expression, we first identified fragment Asp-21–Ser-42 to be functionally important. We then found that deletion mutant Δ1–36 (TRPP3 missing fragment Met-1–Arg-36) has a similar function as wild-type TRPP3, whereas Δ1–38 is functionally dead, suggesting the importance of Val-37 or Cys-38. Further studies found that Cys-38, but not Val-37, is functionally critical. Cys-38 is a predicted site of palmitoylation, and indeed TRPP3 channel activity was inhibited by palmitoylation inhibitor 2-bromopalmitate and rescued by palmitoylation substrate palmitic acid. The TRPP3 N terminus (TRPP3NT, Met-1–Leu-95) localized along the plasma membrane of HEK293 cells but stayed in the cytoplasm with 2-bromopalmitate treatment or C38A mutation, indicating that TRPP3NT anchors to the surface membrane through palmitoylation at Cys-38. By acyl-biotin exchange assays, we showed that TRPP3, but not mutant C38A, is indeed palmitoylated. When putative phosphorylation sites near Cys-38 were mutated to Asp or Glu to mimic phosphorylation, only T39D and T39E reduced TRPP3 function. Furthermore, TRPP3NT displayed double bands in which the upper band was abolished by λ phosphatase treatment or T39A mutation. However, palmitoylation at Cys-38 and phosphorylation at Thr-39 independently regulated TRPP3 channel function, in contrast to previous reports about correlated palmitoylation with a proximate phosphorylation. Palmitoylation at Cys-38 represents a novel mechanism of functional regulation for TRPP3.

Transient receptor potential (TRP)[4] channels are a superfamily of cation channels that play distinct sensory roles in response to a variety of extracellular stimuli, including light, sound, chemicals, temperature, and touch (1). The TRP superfamily has been divided into the following eight subfamilies named after the first identified member in each subfamily: TRPC, TRPV, TRPM, TRPA, TRPN, TRPY, TRPML, and TRP polycystin. Similar to voltage-gated potassium channels, TRP channels were predicted to function as tetramers in which each subunit has six transmembrane helices (TM1–TM6), with a pore loop between TM5 and TM6, and cytosolic N and C termini of varying sizes (2). This structural architecture was confirmed by recently published TRPV1, -2, -6 and TRPA1 structures (3–6).

The founding member of the TRP polycystin subfamily, TRPP2 (also called PKD2 or polycystin-2), is mutated in 15% autosomal dominant polycystic kidney disease (ADPKD), the most common genetic disorder of the kidney, affecting 1 in 400 to 1000 individuals worldwide (7). The remaining ADPKD is caused by mutations in the *PKD1* gene. TRPP3, also called PKD2L1 or polycystin-L, is a homologue of TRPP2 with 50% identity in protein sequence but is not involved in ADPKD. TRPP3 is expressed in bipolar neurons in the tongue taste buds where it presumably plays an important role in sour tastes. Genetic ablation of cells expressing TRPP3 eliminates gustatory nerve response to sour stimuli in mice (8–10). Involvement of TRPP3 in tasting sour was later supported by the report that TRPP3 knock-out mice display a defective ability for tasting acid (11). TRPP3 is expressed in neurons surrounding the central canal of spinal cord where it may be implicated in modulating pH-dependent action potential characteristics (8, 12, 13). TRPP3 is also expressed in brain, kidney, and heart with unknown function (14).

TRPP3 is localized on the surface membrane and/or endoplasmic reticulum membrane, in part depending on the cell type. In *Xenopus laevis* oocytes, TRPP3 targets to the plasma membrane when expressed alone and acts as a Ca^{2+}-activated channel permeable to Na^+, K^+, and Ca^{2+} (15, 16). In human embryonic kidney (HEK) cell lines, TRPP3 mainly targets to the endoplasmic reticulum membrane when expressed alone but traffics to the plasma membrane when co-expressed with PKD1

* This work was supported in part by the Natural Sciences and Engineering Research Council of Canada and National Natural Science Foundation of China Grants 8157041737 (to X. Z. C.) and 81602448 (to J. T.). The authors declare that they have no conflicts of interest with the contents of this article.
[1] Recipient of the Alberta Innovates-Doctoral Graduate Student Scholarship.
[2] To whom correspondence may be addressed. E-mail: jingfeng9930@163.com.
[3] To whom correspondence may be addressed: E-mail: xzchen@ualberta.ca.
[4] The abbreviations used are: TRP, transient receptor potential; PA, palmitic acid; ADPKD, autosomal dominant polycystic kidney disease; TEVC, two-electrode voltage clamp; EGFP, enhanced GFP; 2BP, 2-bromopalmitate; PM, plasma membrane; β2AR, β2-adrenoreceptor; PM, plasma membrane; λPP, λ-phosphatase.

or PKD1L3, a homologue of PKD1 (9, 17, 18). TRPP3 alone, or together with PKD1L3, mediates pH-dependent cation conductance in an off-response manner, *i.e.* activation occurred only after low extracellular pH was removed (9, 19, 53). TRPP3 was also found to be expressed in primary cilium and to regulate ciliary Ca^{2+} concentration and hedgehog signaling (20, 21). Although TRPP3 contains putative phosphorylation, glycosylation, and palmitoylation sites, it is unclear whether and how it is regulated via post-translational modifications. Its homologue TRPP2 channel activity or trafficking was reported to be regulated by phosphorylation at C-terminal Ser-812 by casein kinase II (22) and N-terminal Ser-76 by glycogen synthase kinase 3 (23). Moreover, TRPP2 is also glycosylated but with an unclear functional role (24).

Palmitoylation is a reversible covalent fatty acid modification that attaches the C16 fatty acid palmitate to a cytoplasmic cysteine residue (25). Like other lipid modifications, such as myristoylation and prenylation, palmitoylation serves to tether cytoplasmic proteins to the surface of membranes. In mammals, there are 23 palmitoyltransferases containing a conserved zinc-binding site and Asp-His-His-Cys (DHHC) motif; thus, these enzymes are often referred to as zDHHC-palmitoyltransferases (26, 27). The reversibility of the palmitoylation reaction represents a dynamic regulation mechanism. In some membrane proteins, such as G-protein coupled receptors, palmitoylation of a C-terminal domain has led to the formation of an additional intracellular loop linked to receptor de-sensitization (28–30). An increasing number of ion channel proteins has been reported to undergo palmitoylation as a way of controlling the anchorage of an intracellular domain to membranes (31). An interplay between palmitoylation and phosphorylation has recently been recognized as a new mechanism of regulating the trafficking or function of ion channels (31). Among them, TRPML1 has been reported to undergo palmitoylation and de-phosphorylation, following histamine stimulation of gastric acid secretion, which may underlie the mechanism of its endocytosis (32, 33).

In this study, using *X. laevis* oocyte expression and the two-electrode voltage clamp (TEVC) technique, we first identified the N-terminal residue Cys-38 in human TRPP3 to be critical for its channel function. We then showed that this is mediated through palmitoylation at Cys-38. We also identified Thr-39 to be a functionally important phosphorylation site immediately downstream of Cys-38. Finally, we showed that palmitoylation at Cys-38 and phosphorylation at Thr-39 regulate TRPP3 channel function rather independently, in contrast to other ion channels that are regulated by palmitoylation and correlated phosphorylation at a proximate residue.

Results

Identification of TRPP3 N-terminal Cys-38 Important for Its Channel Function—Our previous report showed the importance of the N terminus of TRPP3 (TRPP3NT, Met-1–Leu-95) for its Ca^{2+}-activated channel activity when expressed in *Xenopus* oocytes (16). Consistently, deletion of TRPP3NT abolished the off-response channel activity of the TRPP3-PKD1L3 complex expressed in HEK cells (34). To determine which domain(s)/residue(s) in TRPP3NT is critical for its channel function, we first generated several truncation mutants, named Δ1–20 (with fragment Met-1–Trp-20 deleted), Δ1–41, Δ1–60, Δ1–81, and Δ1–95 (Fig. 1*A*). When expressed in oocytes, Δ1–20 exhibited similar radiotracer Ca^{2+} transport activity as the wild-type (WT) TRPP3, although the other mutants did not exhibit significant activity (Fig. 1*B*). Consistently, when the whole-cell currents were measured at −50 mV using the TEVC technique, Δ1–20 and WT channels had similar channel function, although the other mutants did not produce any appreciable currents (Fig. 1, *C* and *D*). Similar results were obtained when currents were measured at other membrane potentials using a ramp protocol (Fig. 1*E*). We then performed immunofluorescence assays to examine the surface membrane localization of these mutants and found that these mutations do not significantly affect the surface membrane targeting (Fig. 1*F*). Taken together, these data demonstrate that the Asp-21–Ser-41 fragment is important for TRPP3 channel function.

We next performed further mutations truncating at various positions within Asp-21–Ser-41 and found that the function of Δ1–30 and Δ1–36 is similar to the WT channel, whereas mutants Δ1–38 and Δ1–40 completely lose their function with unaffected surface membrane localization (Fig. 2, *A* and *B*), indicating that residue Val-37 or Cys-38 is important for TRPP3 channel function. We then generated single point mutants V37A, C38A, and double point mutant V37A/C38A and found that only the C38A and V37A/C38A mutations result in substantially reduced channel activity, although the V37A mutation has little effect on channel activity (Fig. 2, *C*–*E*). Biotinylation assays showed that the surface membrane localization is not significantly affected by any of these mutations (Fig. 2*F*). Altogether, these data demonstrate that Cys-38, but not Val-37, is important for TRPP3 channel function.

Palmitoylation of TRPP3 at Cys-38—We next examined the functional role of the other cysteine residues located outside the putative intra-membrane helices, including Cys-69, Cys-70, Cys-74, Cys-210, Cys-223, and Cys-512 (Fig. 3*A*). Mutations of these cysteine residues to alanine did not affect channel function (Fig. 3*B*). Thus, Cys-38, highly conserved among various species (Fig. 3*C*), is the only functionally important cysteine residue outside the putative membrane helices. Of note, based on sequence alignment, TRPP3 Cys-512 and its counterpart in human TRPP2 Cys-631 are both located within the short helix of their TM5–TM6 pore loop. Interestingly, TRPP2 Cys-631 was previously reported to be involved in disulfide bond formation and to be essential for its tetrameric assembly and channel function in HEK cells (35). Because of the presence of reducing cytosolic environments, it is unlikely that Cys-38 forms a disulfide bond with another cysteine residue from the same or a different TRPP3 monomer subunit. We thus wondered how Cys-38 contributes to TRPP3 channel function.

Recently, more and more ion channel proteins, such as the large conductance voltage-gated potassium channel and TRPML1, have been reported to be post-translationally modified by palmitoylation at cysteine residues to regulate channel trafficking and/or function (31–33). We then investigated whether TRPP3 Cys-38 is a palmitoylation site. First, we used palmitoylation prediction program CSS-Palm version 4.0 and found that Cys-38 has the highest palmitoylation score com-

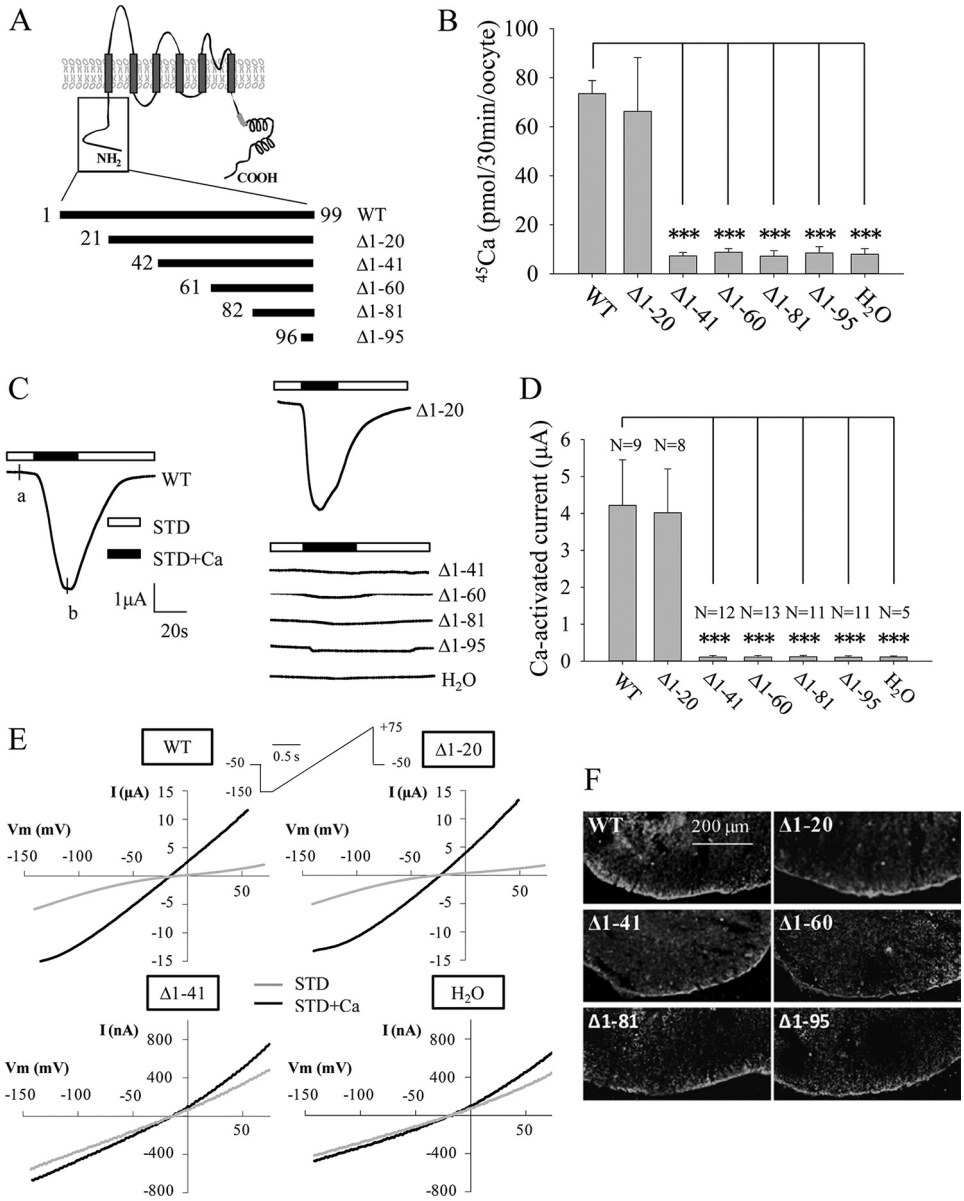

FIGURE 1. **Channel function of human TRPP3 N-terminal truncation mutants.** *A,* putative membrane topology predicted for TRPP3 (*top*) and five truncated mutants with indicated positions of the starting amino acid residue (*bottom*). *B,* radiolabeled ^{45}Ca uptake in *X. laevis* oocytes expressing TRPP3 wild-type (*WT*) or mutants at day 3 following RNA injection. Oocytes injected with H_2O were used as a negative control. Data were averaged from three independent experiments. *** indicates $p < 0.001$. *C,* representative whole-cell current traces obtained from *Xenopus* oocytes expressing TRPP3 WT or an indicated truncation mutant, using TEVC. Oocytes were voltage clamped at −50 mV. Data from H_2O-injected oocytes served as a negative control. Currents were measured using the standard Na^+-containing extracellular solution without (*STD*) or with (*STD+Ca*) 5 mM $CaCl_2$. *D,* averaged Ca^{2+}-activated currents obtained at −50 mV from oocytes expressing TRPP3 WT or an indicated mutant or those injected with H_2O. Currents were averaged from three independent experiments with total numbers of tested oocytes, as indicated. *** indicates $p < 0.001$. *E,* representative current-voltage relationship curves obtained using a voltage ramp protocol, as indicated, before (*STD*) and after (*STD+Ca*) addition of 5 mM $CaCl_2$ at the time point marked with *a* and *b*, respectively, in *C*. *F,* representative immunofluorescence data using oocyte slices, showing expression of TRPP3 WT and indicated truncation mutants.

pared with the other N-terminal cysteine residues, Cys-69, Cys-70, and Cys-74 (Fig. 3*D*). We then treated TRPP3-expressing oocytes with widely used palmitoylation inhibitor 2-bromopalmitate (2BP) (31) overnight at various concentrations from 1 to 50 μM, according to a previous report (36). TRPP3 channel currents measured at −50 mV and other membrane potentials were indeed reduced by 2BP in a dose-dependent manner (Fig. 4, *A–C*). Because immunofluorescence assays found that 2BP treatment has no effect on the TRPP3 plasma membrane expression (Fig. 4*D*), our data showed that 2BP treatment results in an inhibition of TRPP3 channel function in oocytes.

To verify the specificity of the 2BP effect on TRPP3 channel function, we wondered whether the inhibitory effect of 2BP on TRPP3 channel function can be competitively rescued by palmitic acid (PA), the natural substrate of the palmitoylation catalyzed by DHHC enzymes. For this, we treated TRPP3-expressing oocytes overnight with increasing concentrations of PA, from 0 to 20 μM, in the presence of 20 μM 2BP, which inhibited 80% of TRPP3 channel activity (Fig. 4*B*). Indeed, the inhibition of TRPP3 channel activity (measured at −50 mV or other membrane potentials) by 2BP was rescued by PA in a dose-dependent manner (Fig. 5, *A–C*). Again, we confirmed that TRPP3

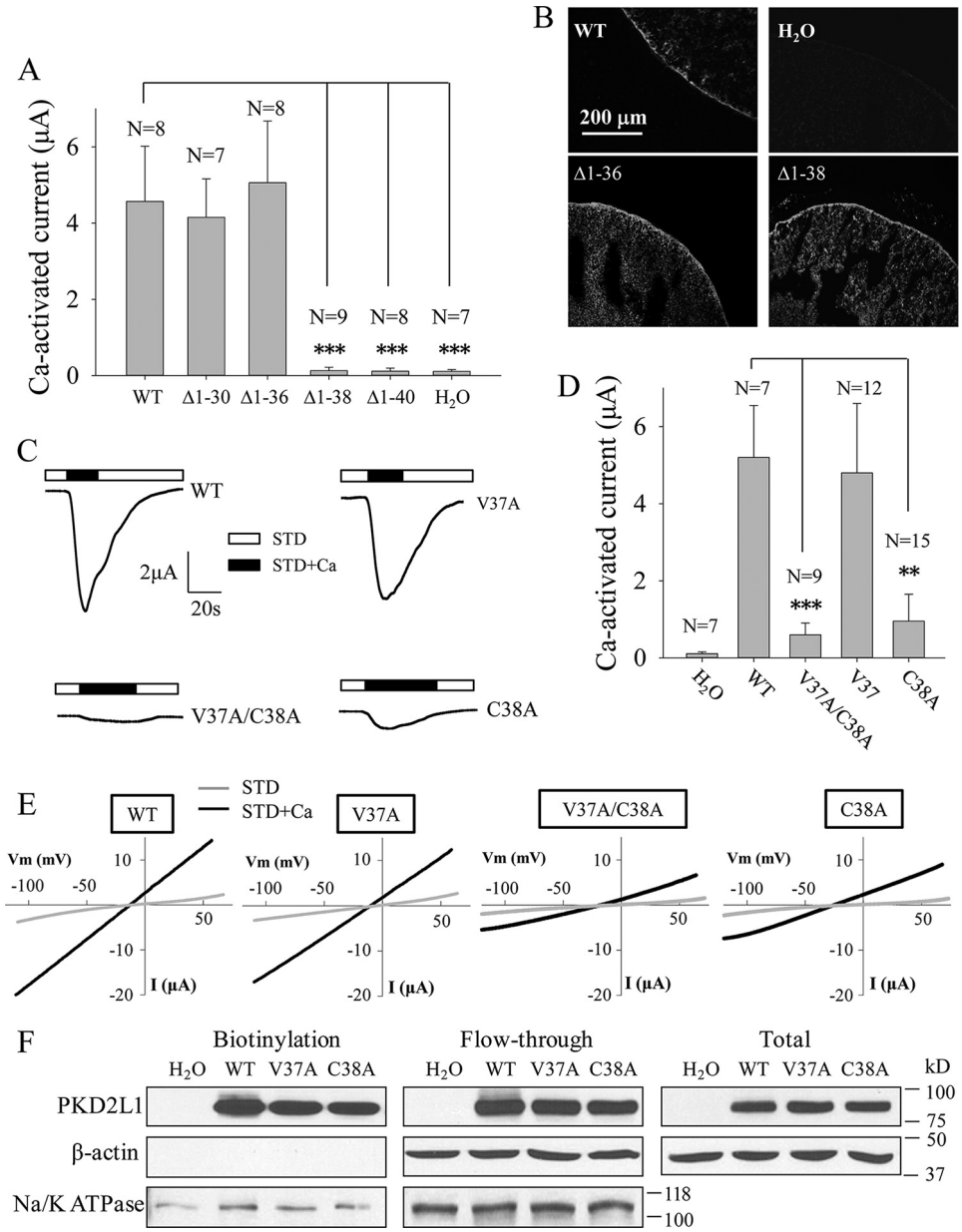

FIGURE 2. **Effects of truncation mutations within Asp-21–Ser-41 and point mutations V37A and C38A on TRPP3 channel function.** *A,* averaged Ca^{2+}-activated currents obtained at −50 mV from oocytes expressing TRPP3 WT or an indicated mutant or from control oocytes (H_2O). Currents were averaged from three independent experiments with indicated total numbers of tested oocytes. *** indicates $p < 0.001$. *B,* representative immunofluorescence data using oocyte slices, showing expression of TRPP3 WT and indicated truncation mutants. H_2O-injected oocytes served as a negative control. *C,* representative whole-cell current traces obtained from oocytes expressing TRPP3 WT, V37A, C38A, or V37A/C38A (double V37A and C38A mutations) using the TEVC technique under similar experimental conditions as those for Fig. 1*C*. *D,* averaged Ca^{2+}-activated currents obtained at −50 mV from oocytes expressing TRPP3 WT, V37A, C38A, or V37A/C38A. Currents were averaged from three independent experiments with indicated total numbers of tested oocytes. ** and *** indicate $p < 0.01$ and 0.001, respectively. *E,* representative current-voltage relationship curves obtained using a voltage ramp protocol, as indicated in Fig. 1*E*, before (*STD*) and after (*STD*+*Ca*) addition of 5 mM $CaCl_2$. *F, left panel,* representative data on the plasma membrane (PM) expression of TRPP3 by biotinylation. Na^+/K^+-ATPase (PM marker) and β-actin (non-PM markers) were used as controls. *Center* and *right panels,* flow-through and total input data, respectively, from the same experiment.

surface membrane localization is not affected by these treatments, as shown by immunofluorescence data in oocytes (Fig. 5*D*). Thus, our rescue experiments using PA supported a specific effect of 2BP on TRPP3 channel function. We also treated TRPP3-expressing oocytes overnight with PA alone, from 1 to 20 μM, but we found no effect on TRPP3 channel activity (Fig. 5*E*), which suggests that there may be a saturated amount of endogenous PA or its equivalent in oocytes. Taken together, these data strongly indicated that TRPP3 is modified by palmitoylation, which is important for TRPP3 channel function, but not trafficking, in *Xenopus* oocytes.

We next wanted to provide further documents on the TRPP3 Cys-38 palmitoylation. It is known that palmitoylation of a transmembrane domain containing protein allows its cytosolic domains to anchor to the plasma membrane (37). We thus examined whether Cys-38 confers palmitoylation and attachment of the N-terminal domain of TRPP3 to the plasma membrane. For this, we overexpressed the EGFP-fused human

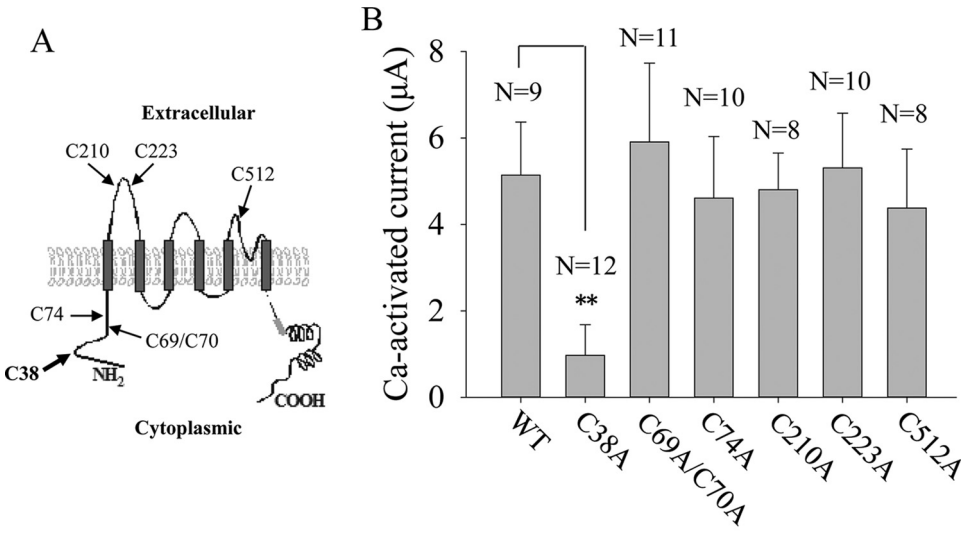

C

C38

Human	21	PHGTLRV**C**TISSTGP	45
Mouse	21	PNRTLRI**C**TVSSVAL	45
Rat	21	PNGTPRI**C**TVSSVAL	45
Monkey	21	PHGTLRV**C**TISSTGP	45
Pig	21	PQEMLRI**C**TISTAAL	45
Rabbit	21	PHGTLRI**C**TISNPVT	45
Cat	21	PHGTLRI**C**TISSVMP	45
Dog	352	PRGTLKI**C**TISSAMP	366

D

CSS-Palm v4.0	Peptide	Position	Score
TRPP3 N-terminus	PHGTLRV**C**TISSTGP	38	8.51
	YRTQVSS**C**CLHICQG	69	5.048
	RTQVSSC**C**LHICQGI	70	5.292
	SSCCLHI**C**QGIRGLW	74	1.676

FIGURE 3. **Characterization of the TRPP3 other intracellular or extracellular cysteine residues and prediction of candidate palmitoylation residues.** *A,* schematic illustration of all intracellular or extracellular cysteine residues in human TRPP3. *B,* averaged Ca^{2+}-activated currents obtained at −50 mV from oocytes expressing TRPP3 WT or an indicated mutant. Currents were averaged from three independent experiments with indicated total numbers of tested oocytes. ** indicates $p < 0.01$. *C,* amino acid sequence alignment of TRPP3 N-terminal fragments containing Cys-38 or the corresponding cysteine from indicated species. National Center for Biotechnology Information accession number for sequences used here are as follows: NP_057196 (human); NP_852087 (mouse); NP_001099822 (rat); XP_001168415 (monkey); XP_012999134 (pig); XP_002718661 (rabbit); XP_006938169 (cat); and XP_005637930 (dog). Potential phosphorylation sites near the cysteine residue are marked with ●. *D,* palmitoylation scores for cysteine residues in the human TRPP3 N terminus predicted by a CSS-palm version 4.0 algorithm. A higher score value indicates a higher probability.

TRPP3 N terminus, Met-1–Leu-95 (EGFP-TRPP3NT) in HEK cells, and detected EGFP epifluorescence to determine TRPP3NT cellular localization using confocal microscopy. We found that EGFP-TRPP3NT indeed shows plasma membrane expression, whereas EGFP-TRPP3CT (a TRPP3 C-terminal fragment, Glu-706–Ser-805, as a negative control) exhibits intracellular distribution only (Fig. 6*A*). As expected, EGFP-N-Ras (a positive control), a well known palmitoylated oncoprotein, also attached to the plasma membrane in our experimental condition (Fig. 6*A*), consistent with its previously reported plasma membrane localization in COS-7 cells (38). To determine whether the plasma membrane expression of EGFP-TRPP3NT is due to palmitoylation, we attempted to disrupt palmitoylation by starving HEK cells in a fatty acid-free medium or treating cells with the palmitoylation inhibitor 2BP (100 μM) overnight, as reported previously (38). Under both conditions, EGFP-TRPP3NT was found to stay in the cytoplasm (Fig. 6*B*), indicating that palmitoylation is required for the plasma membrane targeting of TRPP3NT. Similar results were also obtained for EGFP-N-Ras (Fig. 6*B*), which is consistent with the previous report using COS-7 cells (38). Furthermore, C38A mutation also resulted in localization of EGFP-TRPP3NT in the cytoplasm (Fig. 6*B*).

We next performed acyl-biotin exchange assays to directly determine whether TRPP3 is palmitoylated. For this, we transiently transfected FLAG-tagged TRPP3 WT and mutants

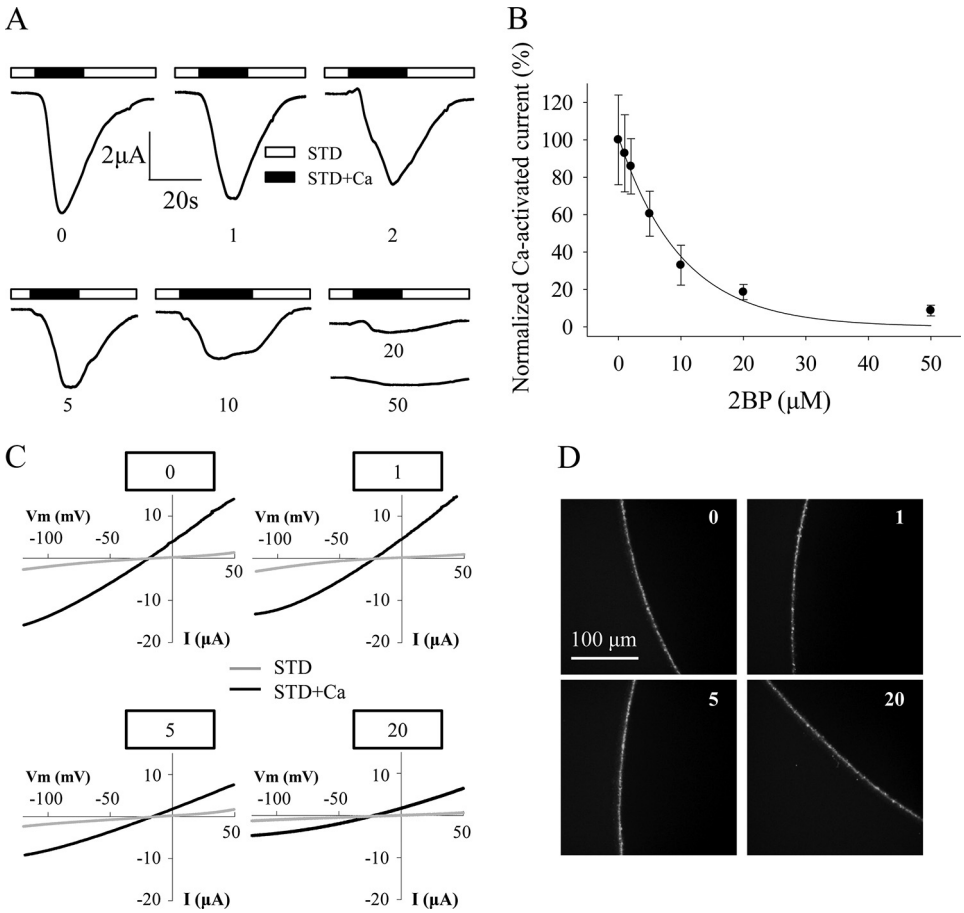

FIGURE 4. **Effect of palmitoylation inhibitor 2BP on TRPP3 channel activity.** *A,* representative whole-cell current traces obtained at −50 mV from oocytes expressing TRPP3 and treated with DMSO (0.05% in Barth's solution) dissolving different concentrations of 2BP (in μM, 0, 1, 2, 5, 10, 20, and 50) overnight before current measurements with the TEVC. *B,* averaged Ca^{2+}-activated currents obtained at −50 mV from oocytes expressing TRPP3 under similar treatments as those in *A* to show concentration-dependent inhibition of Ca^{2+}-activated TRPP3 channel activity by 2BP. Currents were averaged from three independent experiments and normalized to that of TRPP3-expressing oocytes without 2BP treatment. *C,* representative current-voltage relationship curves obtained using a voltage ramp protocol before (*STD*) and after (*STD+Ca*) addition of 5 mM $CaCl_2$. Oocytes expressing TRPP3 were incubated with indicated concentrations of 2BP. *D,* representative whole-mount immunofluorescence data showing the PM expression of TRPP3 WT in oocytes treated with indicated concentrations of 2BP.

C38A and T39E in HEK cells. TRPP3 was first immunoprecipitated with a rabbit anti-FLAG antibody and protein G-coated Sepharose beads. Immunoprecipitated TRPP3 proteins were then treated either with hydroxylamine to remove palmitate or with Tris base as a negative control. The exposed cysteine thiol groups were labeled with a thiol-reactive biotinylation reagent, 1-biotinamide-4[4′(maleimidomethyl)cyclohexane-carboxamido] butane (biotin-BMCC). The streptavidin-HRP antibody was then used to detect the palmitoylated TRPP3 and a mouse anti-FLAG antibody to detect total immunoprecipitated TRPP3. We indeed found that TRPP3 and mutant T39E, but not mutant C38A, are modified by palmitoylation (Fig. 6*C*). Furthermore, the TRPP3 palmitoylation was abolished by 2BP treatment overnight at a concentration of 100 μM (Fig. 6*C*). These data together demonstrated that TRPP3 is indeed palmitoylated at Cys-38, which accounts for our observation that the plasma membrane targeting of TRPP3NT requires palmitoylation at Cys-38. Interestingly, the N terminus of TRPP2 (EGFP-TRPP2NT, Met-1–Lys-215) that possesses four cysteine residues also targeted to the plasma membrane when overexpressed in HEK cells, although the C terminus of TRPP2 (EGFP-TRPP2CT, Asp-682–Val-968) showed a cytosolic distribution (Fig. 6*D*), suggesting that the N-terminal palmitoylation is a shared mechanism by TRPP3 and TRPP2.

Phosphorylation of TRPP3 at Thr-39—Because there have been reports about an interplay between palmitoylation and phosphorylation at a nearby site (37, 39, 40), we next examined potential phosphorylation sites near Cys-38. Five candidate phosphorylation sites, Thr-34, Thr-39, Ser-41, Ser-42, and Thr-43 are predicted in human TRPP3 by GPS 3.0 program (Fig. 3*C*). First, mutating any of these five sites to alanine did not affect channel function (41), suggesting either that these sites are not important or that expressed TRPP3 channels on the surface membrane are predominantly de-phosphorylated at one of these sites in *Xenopus* oocytes. We then mutated each of them to Glu to mimic phosphorylation and found that only mutation T39E significantly affects (substantially reduces) the channel function, although no mutation significantly alters the surface membrane localization (Fig. 7, *A* and *B*). Together with our observation that mutant T39D, compared with T39E, exhibited similarly impaired channel function and similar surface membrane localization (Fig. 7, *A* and *B*), our data suggest that Thr-39 is a functionally important phosphorylation site,

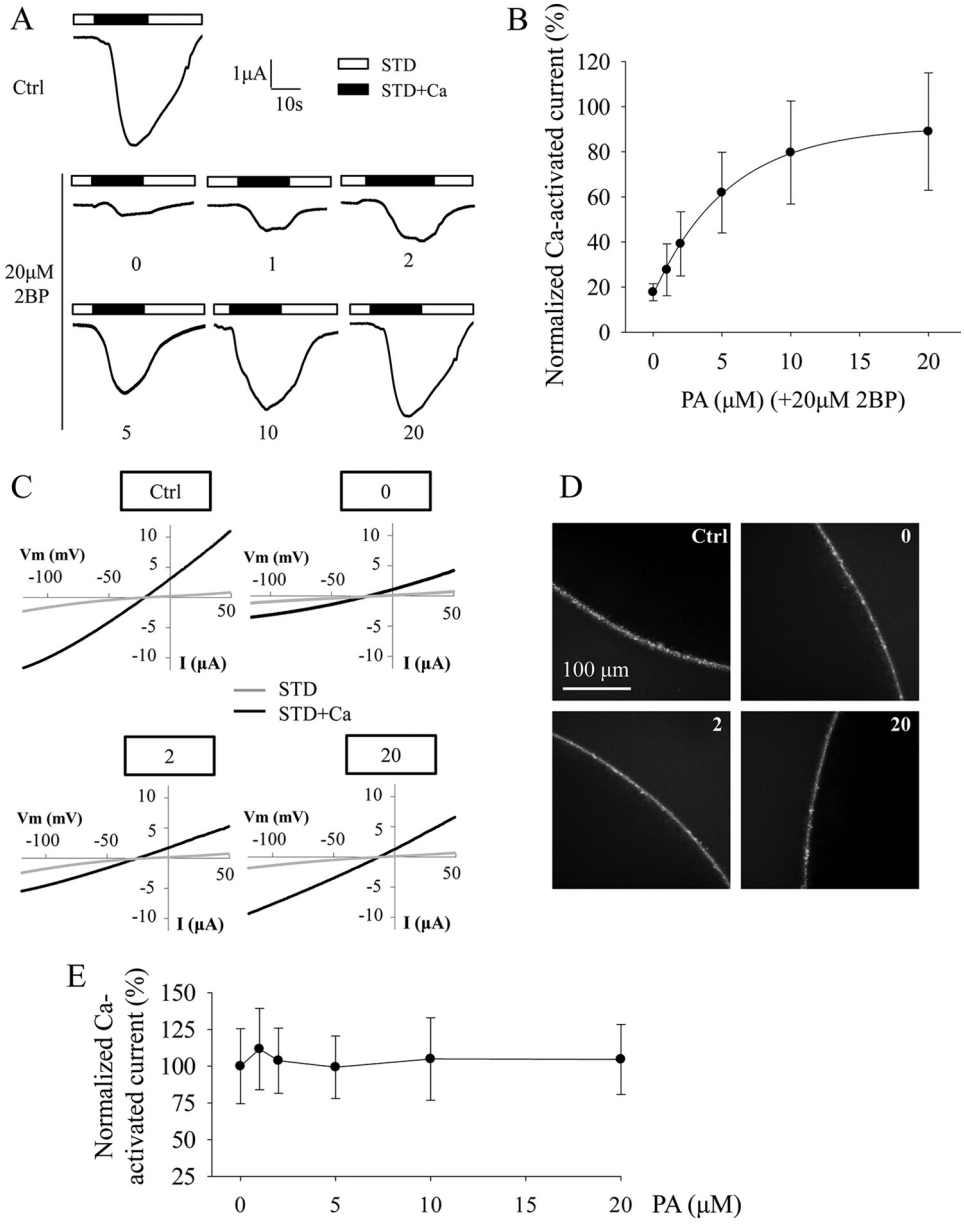

FIGURE 5. **Rescuing effect of PA on 2BP-mediated TRPP3 channel activity inhibition.** *A,* representative whole-cell current traces obtained at −50 mV from oocytes expressing TRPP3 and treated with different concentrations of PA (in μM, 0, 1, 2, 5, 10, and 20) in the presence of 20 μM 2BP overnight before current measurements with TEVC technique. The TRPP3-expressing oocytes treated with DMSO (0.1% in Barth's solution) were designated as *Ctrl*. *B,* averaged Ca^{2+}-activated currents obtained at −50 mV from oocytes expressing TRPP3 under similar treatments as those in *A* to show concentration-dependent rescue of 2BP-elicited TRPP3 channel activity inhibition by PA. Currents were averaged from three independent experiments and normalized to that of *Ctrl* (0.1% DMSO in Barth's solution). *C,* representative current-voltage relationship curves obtained using a voltage ramp protocol before (*STD*) and after (*STD+Ca*) addition of 5 mM $CaCl_2$. Oocytes expressing TRPP3 were similarly treated as in *A*. *D,* representative whole-mount immunofluorescence data showing the PM expression of TRPP3 in oocytes similarly treated as in *A*. *E,* effect of PA on TRPP3 channel activity. Oocytes expressing TRPP3 were treated with different concentrations of PA (in μM, 0, 1, 2, 5, 10, and 20) overnight before current measurement. Currents were normalized to the values with 0 PA.

which is consistent with the fact that Thr-39 is conserved among different species (Fig. 3*C*).

We next further examined Thr-39 phosphorylation by Western blotting using human TRPP3NT with an N-terminal HA tag. When HA-TRPP3NT was transiently expressed in HEK cells, double bands were observed (Fig. 7*C*, *left panel*). The upper band disappeared following treatment by λ-phosphatase (λPP) (Fig. 7*C*, *left panel*), which removes all phosphate groups from serine, threonine, and tyrosine residues. As a positive control, we found that human TRPP2NT, previously reported to be phosphorylated at Ser-76 (23), also displays double bands under our experimental conditions and that the upper band disappears by the λPP treatment (Fig. 7*C*, *right panel*). Furthermore, mutation of Thr-39 to Ala, but not Ser-41 to Ala, eliminated the upper band of TRPP3NT (Fig. 7*D*). Taken together, our data indicate that TRPP3 is phosphorylated at the N-terminal Thr-39.

Relationship between Palmitoylation at Cys-38 and Phosphorylation at Thr-39—We next investigated whether there is a correlation between palmitoylation at Cys-38 and phosphorylation at Thr-39 of TRPP3, given the presence of an interplay between these two types of post-translational modifications in some membrane proteins (31, 39, 40, 42). For this, we examined

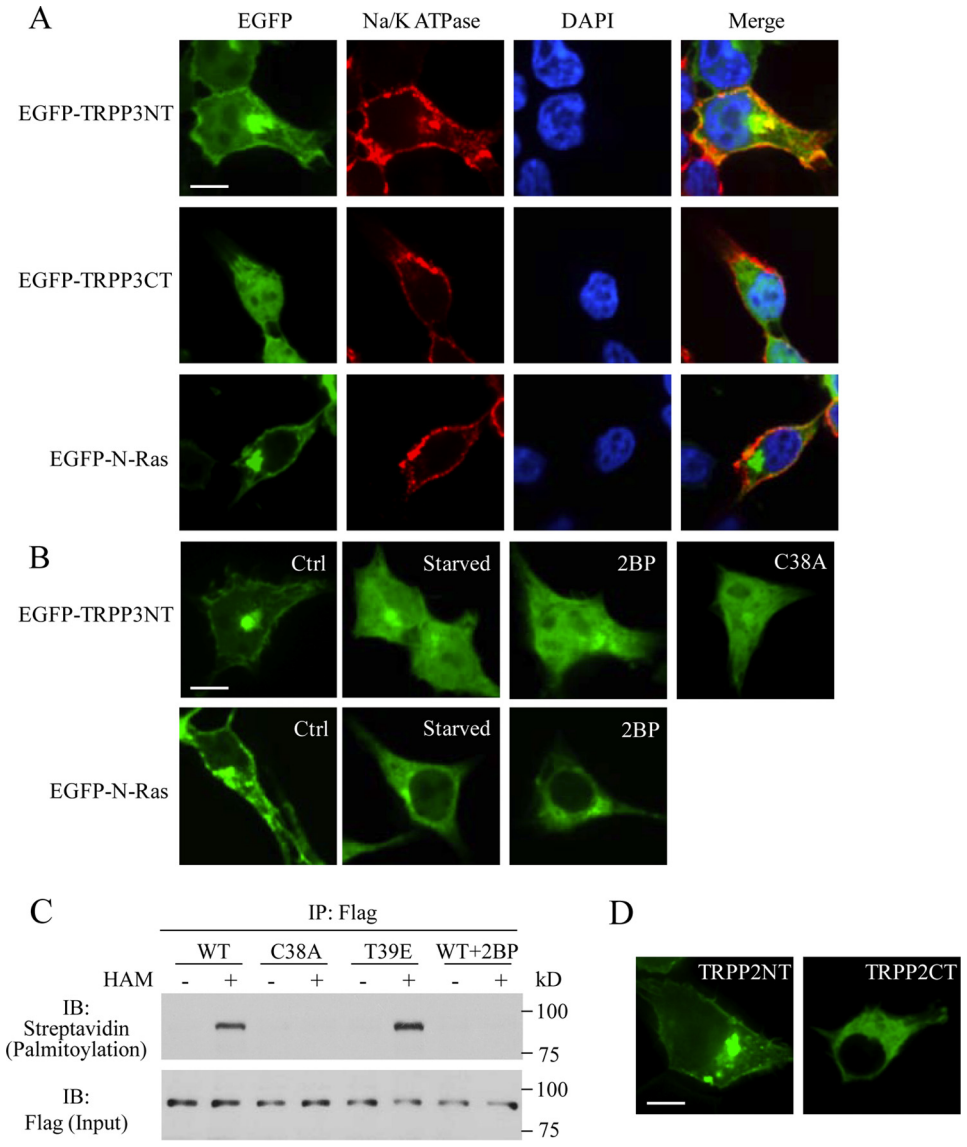

FIGURE 6. **Effects of 2BP and mutation C38A on the plasma membrane anchorage of TRPP3NT and palmitoylation of TRPP3 at Cys-38.** *A,* representative confocal images showing subcellular localization of EGFP-TRPP3NT (EGFP fused the TRPP3 N terminus, Met-1–Leu-95), EGFP-TRPP3CT (EGFP fused the TRPP3 C-terminal fragment Glu-706–Ser-805, as a negative control), and EGFP-N-Ras (EGFP fused with human N-Ras, as a positive control) in HEK cells. *Scale bar,* 10 μm. *B,* subcellular localization of EGFP-TRPP3NT and EGFP-N-Ras in HEK cells without (*Ctrl*) or with fatty acid starvation, with 100 μM 2BP treatment overnight, or with the C38A mutation. *Scale bar,* 10 μm. *C,* palmitoylation of FLAG-TRPP3 in HEK cells detected by immunoprecipitation (*IP*) acyl-biotin exchange assays. See under "Experimental Procedures" for method details. Cells were transfected with WT FLAG-tagged TRPP3 and mutant C38A or T39E. 2BP treatment was as in *B*. Palmitoylated TRPP3 proteins were detected with streptavidin-HRP antibody, and total immunoprecipitated TRPP3 proteins (*Input*) were detected with FLAG antibody. Shown are representative immunoblots (*IB*) from three independent experiments. *D,* representative confocal images showing subcellular localization of EGFP-TRPP2NT (EGFP fused the TRPP2 N terminus, Met-1–Lys-215) and EGFP-TRPP2CT (EGFP fused theTRPP2 C terminus, Asp-682–Val-968) in HEK cells. *Scale bar,* 10 μm.

whether the C38A mutation or Cys-38 de-palmitoylation reduces TRPP3 channel activity through increasing phosphorylation at Thr-39. First, introduction of the C38A mutation to the WT and T39A mutant channels resulted in similar reduction of channel activity (Fig. 8*A*). Second, treatment of oocytes expressing mutant T39A or WT TRPP3 with 20 μM 2BP resulted in similar reduction of channel activity (Fig. 8*A*). As these mutations and 2BP treatments did not significantly affect surface membrane expression (Fig. 8*B*), we concluded that reduction of TRPP3 channel activity by de-palmitoylation is not through increasing phosphorylation at Thr-39. This conclusion was supported by our observation that C38A has little effect on the upper band of TRPP3NT (Fig. 8*C*).

Conversely, we examined whether the T39E mutation, which mimics phosphorylation at Thr-39, reduces TRPP3 channel activity through decreasing palmitoylation at Cys-38. Introduction of the T39E mutation to C38A mutant that cannot be palmitoylated further significantly reduced TRPP3 channel activity (Fig. 8*D*) without affecting plasma membrane expression (Fig. 8*B*), indicating that inhibition of TRPP3 channel function by phosphorylation at Thr-39 is not through decreasing palmitoylation at Cys-38. Furthermore, the T39E mutation had little effect on the plasma membrane localization of TRPP3NT (Fig. 8*E*) and palmitoylation of full-length TRPP3 at Cys-38 (Fig. 6*C*). Taken together, these data showed that TRPP3 channel activity is regulated by palmitoy-

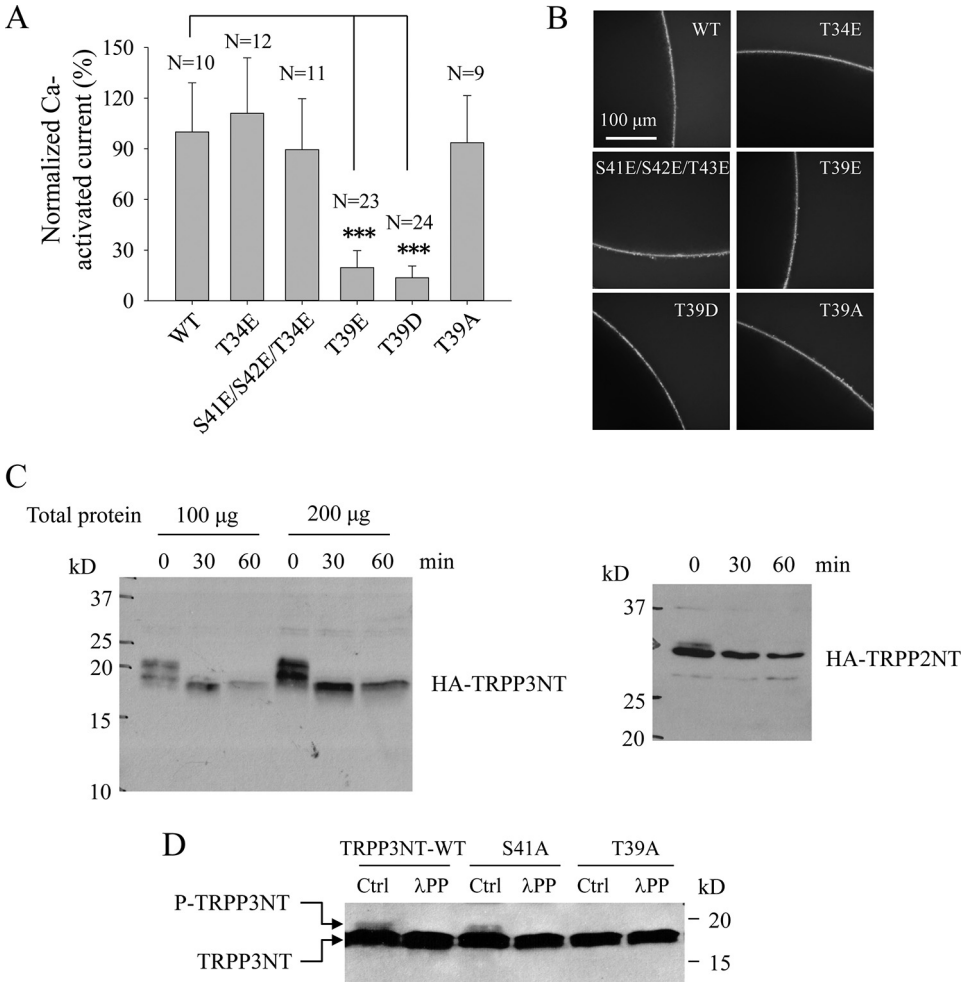

FIGURE 7. **Roles of Thr-39 and its phosphorylation in regulating TRPP3 channel function.** *A,* averaged currents obtained from oocytes expressing TRPP3 WT, T34E, S41E/S42E/T43E (triple S41E, S42E, and T43E mutations) and T39E, T39D, or T39A. Currents at − 50 mV were averaged from three independent experiments with indicated total numbers of tested oocytes and normalized to that of TRPP3 WT. *** indicates $p < 0.001$. *B,* representative whole-mount immunofluorescence data showing the PM expression of TRPP3 WT or a mutant in oocytes. *C,* phosphorylation state of the TRPP3 N terminus assessed by λPP treatment. HA-tagged TRPP3NT and TRPP2NT (as a positive control) were transfected into HEK cells where cell lysates were treated with λPP for the indicated periods of time. Shown are representative blots from three independent experiments. *D,* phosphorylation of TRPP3NT WT and TRPP3NT containing the S41A or T39A mutation. These three constructs were transfected into HEK cells, and resulting cell lysates were treated without (*Ctrl*) or with λPP for 30 min. Shown are representative blots from three independent experiments.

lation at Cys-38 and phosphorylation at Thr-39 rather independently.

Discussion

So far, not much is known about TRPP3 post-translational modifications, although its homologue TRPP2 was reported to undergo phosphorylation, glycosylation, and disulfide bond formation (22, 24, 35). In this study, we found that TRPP3 is modified by palmitoylation and phosphorylation at the N-terminal cysteine 38 and threonine 39, respectively, and showed that these two post-translational modifications independently regulate TRPP3 channel function.

Palmitoylation is a dynamic post-translational modification that was first described 35 years ago in a transmembrane glycoprotein of vesicular stomatitis virus (43). 8 years later, in 1987, the first palmitoylated ion channel, rodent voltage-gated Na^+ channel, was characterized (44). Since then, more than 50 different ion channels have been experimentally demonstrated to be palmitoylated (31). Increasing evidence has so far indicated that palmitoylation may regulate either the channel's membrane density or single channel activity (31). In the case of TRPP3, palmitoylation at Cys-38 had little effect on its plasma membrane expression, at least in *Xenopus* oocytes (Fig. 2*F*), but it dramatically reduced the channel activity (Fig. 2*D*) by a to-be-identified mechanism that is independent of phosphorylation at Thr-39. A surprising characteristic of TRP channels is that they can be activated by a wide variety of environmental stimuli. A shared mechanism underlying gating of TRPs by seemingly disparate activators was recently proposed by Liu and Montell (45) based on the discovery that a phospholipase C-dependent signaling cascade activates TRP channels in *Drosophila* photoreceptor cells through generation of force in the lipid bilayer. According to this theory, besides known mechano-sensitive TRP channels, other TRPs are also activated through mechanical forces formed by architectural changes in the cell membrane in response to different stimuli (45). TRPP2 was known to be co-localized with PKD1 in primary cilia of kidney cells where it is believed to act as part of a mechanical sensor (46). In con-

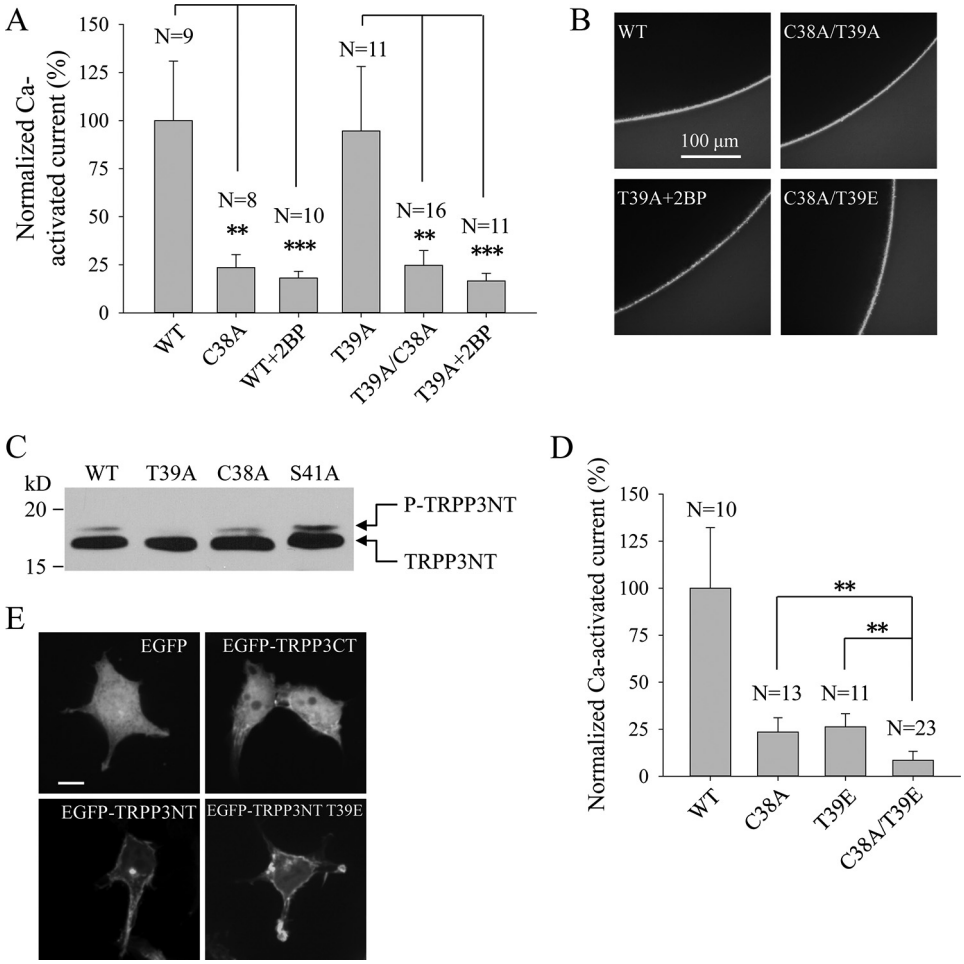

FIGURE 8. **Relationship between palmitoylation at Cys-38 and phosphorylation at Thr-39.** *A,* averaged Ca^{2+}-activated currents obtained at −50 mV from oocytes expressing TRPP3 WT without or with 20 μM 2BP treatment (*WT+2BP*), C38A, T39A, without or with 20 μM 2BP treatment (*T39A+2BP*), or C38A/T39A (double C38A and T39A mutations). Currents were averaged from three independent experiments with indicated total numbers of tested oocytes and normalized to that of TRPP3 WT. ** and *** indicate $p < 0.01$ and 0.001, respectively. *B,* representative whole-mount immunofluorescence data showing the PM expression of TRPP3 WT, C38A/T39A, C38A/T39E, and T39A with 20 μM 2BP treatment (*T39A+2BP*). *C,* phosphorylation of TRPP3NT WT and TRPP3NT with the T39A, C38A, or S41A mutation in HEK cells. *D,* averaged and normalized currents obtained at −50 mV from oocytes expressing TRPP3 WT, C38A, T39E, or C38A/T39E. Currents were averaged from three independent experiments with indicated total numbers of tested oocytes and normalized to that of TRPP3 WT. ** indicates $p < 0.01$. *E,* representative confocal images showing subcellular localization of EGFP, EGFP-TRPP3CT, EGFP-TRPP3NT, and EGFP-TRPP3NT T39E in HEK cells. *Scale bar,* 10 μm.

trast, TRPP3 was reported to be co-localized with PKD1L1 in cilia (20) even though it remains unclear as to whether it is mechano-sensitive. It is generally assumed that palmitoylation facilitates the association of the protein to the membrane. Therefore, it is possible that TRPP3 palmitoylation has an interplay with the mechanical force exercised on the cell membrane with respect to channel gating. Alternatively, it remains to be determined whether palmitoylation regulates TRPP3 channel activity through facilitating an intramolecular interaction between its N-terminal pre-S1 and C-terminal TRP domains. This type of interaction was suggested to occur in TRPV1, TRPV2, TRPA1, and TRPV6 based on structural information revealed using cryo-EM or crystallography (3–6).

TRPP3 is expressed in the brain (14), and a recent study using TRPP3 knock-out mice found that disruption of TRPP3 causes hippocampal and thalamocortical hyperexcitability and increases susceptibility to pentylenetetrazol-induced seizures (47). Interestingly, several neural proteins, including various G-protein-coupled receptors and ion channels that control the excitability of neurons, have now been reported to be dynamically regulated by palmitoylation (48). It would be interesting to see whether palmitoylation of TRPP3 at Cys-38 represents a mechanism underlying the control of TRPP3 channel activity in neurons with respect to neuronal excitability. TRPP3 was also found to interact with β2-adrenoreceptor (β2AR) and co-localize with β2AR in the brain (47). Binding of agonist isoproterenol to β2AR was reported to markedly reduce the palmitoylation of the associated $G\alpha_s$ (49). Thus, it is possible that β2AR regulates TRPP3 palmitoylation through physical binding. Furthermore, β2AR itself is also palmitoylated, and agonist-stimulated de-palmitoylation of β2AR was reported to promote its phosphorylation and β-arrestin-mediated receptor internalization (28). Therefore, it would be interesting to see whether there is an interplay between TRPP3 palmitoylation and β2AR, how this interplay is regulated, and whether it is involved in the control of neuronal excitability.

Post-translational modifications of TRP channels, such as glycosylation, phosphorylation, and covalent/reversible bind-

ing of an activator to a cysteine residue, mainly affect their subcellular trafficking or channel activity (50). To date, within the TRP superfamily only, TRPML1 is known to be palmitoylated, both in a heterologous expression system and native stomach tissue, for regulation of its endocytosis (32, 33). Thus, TRPP3 represents the first TRP member whose channel function is regulated by palmitoylation. It would thus be important to examine whether the function of other TRPs is also regulated by palmitoylation and to investigate the physiological implications of this type of post-translational modification. Palmitoylation is mostly mediated by a family of 23 (human) DHHC motif-containing palmitoyltransferases with unclear substrate specificities (37). De-palmitoylation, however, is mediated by acylprotein thioesterases (APTs), including APT1, APT2, and APT-like (37). Future studies would have to determine which DHHC enzyme(s) and acylprotein thioesterases are involved in TRPP3 palmitoylation and de-palmitoylation.

Phosphorylation at the C-terminal Ser-812 of TRPP2 by casein kinase II regulates its channel function, whereas phosphorylation at the N-terminal Ser-76 by glycogen synthase kinase 3 regulates its subcellular localization (22, 23). Although phosphorylation of TRPP3 at the N-terminal Thr-39 abolishes its channel function, we still do not know which kinase is involved. Prediction by GPS 3.0 program suggests that a PKC kinase phosphorylates TRPP3 at Thr-39. Of note, the fact that mutant T39A displayed a similar functional activity as the WT channel suggests that TRPP3 channels in oocytes are mostly de-phosphorylated, which is consistent with our data obtained from Western blotting experiments (Fig. 7*D*). It is also interesting to determine whether TRPP3 is phosphorylated at other sites and, if any, what are the corresponding functional roles. Furthermore, although palmitoylation at Cys-38 and phosphorylation at Thr-39, the only phosphorylation site proximate to Cys-38, are both functionally important for TRPP3, our experiments showed that they are not linked to each other. This is in contrast to previously reported ion channels with respect to an interplay between the two modifications. For example, large conductance Ca^{2+}- and voltage-gated K^+ channels were found to be inhibited by PKA phosphorylation of a C-terminal serine residue, immediately upstream of a conserved palmitoylated cysteine residue, by reducing palmitoylation to disrupt the anchorage of their C terminus to the plasma membrane (39). Thus, it could be that TRPP3 palmitoylation at Cys-38 is not linked to any phosphorylation or to a phosphorylation that is not close to Cys-38, which would suggest that TRPP3 palmitoylation may represent a novel and yet-to-be determined way of functional regulation. Because both phosphorylation and palmitoylation are of dynamic and reversible regulation mechanisms, it would be important to elucidate how the function of other TRPs is regulated by the two modifications and to examine potential cross-talk between them.

In summary, this study has identified N-terminal Cys-38 as a palmitoylation site that mediates anchorage of the N terminus to the surface membrane and regulates TRPP3 channel function. We have also identified N-terminal Thr-39 as a phosphorylation site critical for TRPP3 channel function. Furthermore, we have shown that the palmitoylation and phosphorylation independently regulate TRPP3 channel function, which we think may represent a novel mechanism of regulation that deserves further studies.

Experimental Procedures

Vectors, Plasmids, and Antibodies—Human full-length TRPP3 cDNA was subcloned into vector pCHGF (41) for *X. laevis* oocyte expression. FLAG tag was then inserted 5′ of the TRPP3 coding region for detection. cDNAs coding for the N or C termini of human TRPP3 and TRPP2 were subcloned into the pEGFPC2 vector for mammalian cell expression. All mutations were made with QuikChange Lightning Site-directed Mutagenesis kit (Agilent Technologies, La Jolla, CA) and confirmed by sequencing. Rabbit antibodies against FLAG (D-8), Na^+/K^+-ATPase (H-300), and mouse antibodies against β-actin (C-4) were purchased from Santa Cruz Biotechnology (Santa Cruz, CA). Mouse antibody against HA (HA.C5) was purchased from Abcam (Cambridge, MA). Secondary antibodies were purchased from GE Healthcare.

Preparation of mRNAs and Microinjection into Oocytes—pCHGF plasmids containing TRPP3 WT or mutant cDNAs were linearized with MluI, followed by phenol/chloroform purification and ethanol precipitation. Linearized DNAs were then used to *in vitro* synthesize capped mRNAs using mMESSAGE mMACHINE kit (Ambion, Austin, TX). Stage V–VI oocytes were isolated from *X. laevis*. Defolliculation of oocytes was performed through incubation in Ca^{2+}-free Barth's solution (51) containing collagenase (2 mg/ml) at room temperature for 1 h. Oocytes were then incubated at 18 °C in the Barth's solution for at least 3 h before injection of 25 nl of RNase-free water containing 25 ng of mRNAs using picospritzer III (Parker Hannifin, Cleveland, OH). An equal volume of water was injected into each control oocyte. This study was approved by the Ethical Committee for Animal Experiments of the University of Alberta and was carried out in accordance with the Guidelines for Research with Experimental Animals of the University of Alberta and the Guide for the Care and Use of Laboratory Animals (National Institutes of Health Guide) revised in 1996. Injected oocytes were incubated at 18 °C in the Barth's solution supplemented with antibiotics for 2–4 days prior to experiments.

^{45}Ca Uptake—Radiotracer uptake experiments were performed as described previously (15). In brief, radioactive $^{45}CaCl_2$ (Amersham Biosciences, UK) at 30 μM was added to the uptake solution (100 mM *N*-methyl-D-glucamine, 2 mM KCl, 1 mM $MgCl_2$, 10 mM HEPES, pH 7.5) plus 1 mM non-radioactive $CaCl_2$. Ten oocytes of each sample were incubated in 0.5 ml of the uptake solution for 30 min, and the incubation was terminated by washing oocytes with ice-cold NaCl-containing solution (100 mM NaCl, 2 mM KCl, 1 mM $MgCl_2$, 10 mM HEPES, pH 7.5). Individual oocytes were then dissolved in 250 μl of 10% SDS and mixed with 2.5 ml of scintillation mixture prior to scintillation counting.

Two-electrode Voltage Clamp—TEVC experiments were performed as described before (41). Briefly, the two electrodes (capillary pipettes, Warner Instruments, Hamden, CT) impaling an oocyte were filled with 3 M KCl to form a tip resistance of 0.3–2 megohms. The standard extracellular solution containing 100 mM NaCl, 2 mM KCl, 1 mM $MgCl_2$, and 10 mM HEPES,

pH 7.5, with or without 5 mM $CaCl_2$ was used. The duration of application of Ca^{2+} solution was indicated in time course recordings. The palmitoylation inhibitor 2BP (Sigma) was made as a fresh 100 mM stock in DMSO and applied at various concentrations from 1 to 50 μM overnight. Oocyte whole-cell currents were recorded using a Geneclamp 500B amplifier and Digidata 1322A AD/DA converter (Molecular Devices, Union City, CA). The pClamp 9 software (Axon Instruments, Union City, CA) was employed for data acquisition and analysis. Currents and voltages were digitally recorded at 200 μs/sample and filtered at 2 kHz through a Bessel filter. SigmaPlot 12 (Systat Software, San Jose, CA) was used for data fitting and plotting.

Oocyte Immunofluorescence—Immunofluorescence assays using oocyte slices were performed as described previously (41). Whole-mount staining was performed as follows: *Xenopus* oocytes were washed in PBS, fixed in 4% paraformaldehyde for 15 min, washed three times in PBS plus 50 mM NH_4Cl, and then permeabilized with 0.1% Triton X-100 for 4 min. Oocytes were then blocked in PBS plus 3% skim milk for 30 min, and then incubated overnight with the rabbit anti-TRPP3 polyclonal antibody (catalog no. PAB5914, Abnova, Taiwan), followed by incubation with a secondary AlexaFluor 488-conjugated donkey anti-rabbit antibody (Jackson ImmunoResearch, West Grove, PA) for 30 min. Oocytes were then mounted in Vectashield (Vector Labs, Burlington, Ontario, Canada) and examined on an AIVI spinning disc confocal microscopy (Cell Imaging Facility, Faculty of Medicine and Dentistry, University of Alberta).

Western Blotting—Protein samples were prepared with CelLytic M lysis buffer (Sigma) from oocytes or mammalian cells according to the manufacturer's instruction. 50–80 μg of total proteins were then separated on 8% SDS-polyacrylamide gels and transferred to nitrocellulose membranes that were then blocked for 1 h at room temperature with 3% skim milk in PBS buffer supplemented with 1% Tween 20. This was followed by overnight incubation at 4 °C with diluted primary antibodies in blocking buffer according to suppliers' suggestions. Secondary horseradish peroxidase-coupled anti-mouse and anti-rabbit antibodies were purchased from GE Healthcare.

Biotinylation—*Xenopus* oocytes were washed three times with PBS followed by incubation with 0.5 mg/ml sulfo-NHS-SS-Biotin (Pierce) for 30 min at room temperature. 1 M NH_4Cl was used to quench the non-reacted biotin. Oocytes were then washed with PBS and harvested in ice-cold CelLytic™ M lysis buffer (Sigma) supplemented with proteinase inhibitor mixture (Thermo Scientific, Waltham, MA). Lysates were incubated at room temperature for 3 h with gentle shaking upon addition of 100 μl of streptavidin (Pierce). The surface protein absorbed by streptavidin was resuspended in SDS and subjected to SDS-PAGE.

Mammalian Cell Culture, Transfection, and Treatments—HEK293 cells were cultured in Dulbecco's modified Eagle's medium (DMEM) supplemented with 10% fetal bovine serum (FBS) and 1% penicillin/streptomycin (Sigma). Transient transfection was performed using Lipofectamine 2000 (Invitrogen) according to the manufacturer's instruction. The palmitoylation inhibitor 2-BP (Sigma) was made as a fresh 100 mM stock in DMSO and applied at a final concentration of 100 μM overnight. For fatty acid starvation, cells were incubated overnight with DMEM supplemented with 10% FBS treated with 5% dextran-coated charcoal (Sigma).

Confocal Imaging—Transfected HEK cells were washed in PBS and fixed in 4% paraformaldehyde for 15 min followed by permeabilization in 0.1% Triton X-100 for 15 min at room temperature. Cells were then blocked with 3% bovine serum albumin in PBS for 30 min. Where indicated, cells were stained with mouse antibody against Na^+/K^+-ATPase (catalog no. ab7671, Abcam) or rat 1:200 dilution for 1 h at room temperature, followed by incubation with a secondary Cy3-conjugated goat anti-mouse antibody (Jackson ImmunoResearch) for 30 min. Cells were then mounted in ProLong® Diamond Antifade Mountant with DAPI (Molecular Probes, Eugene, OR) and examined on an AIVI spinning disc confocal microscopy (University of Alberta).

Acyl-Biotin Exchange Assay—Transfected or treated HEK cells were washed three times in PBS and lysed in 500 μl of lysis buffer (LB, 1% IGEPAL CA-630, 50 mM Tris-HCl, pH 7.5, 150 mM NaCl, and 10% glycerol) supplemented with protease inhibitor mixture (Thermo Scientific) and 50 mM freshly made *N*-ethylmaleimide (Thermo Scientific). Acyl-biotin exchange experiments were performed as described previously (52). In brief, proteins were immunoprecipitated with rabbit anti-FLAG antibody (catalog no. ab1162, Abcam) and 50% slurry of protein G-coated Sepharose beads (GE Healthcare). After washing three times with LB supplemented with 0.1% SDS, each sample of beads was split into two with one incubated with 500 μl of LB, pH 7.2, and the other with the same volume of LB containing 1 M hydroxylamine (Sigma) to cleave the thioester bond. The samples were rotated at room temperature for 1 h. After the beads were washed once in LB, pH 6.2, the samples were incubated with 3 μM biotin-BMCC (Thermo Scientific) in LB, pH 6.2, to label the unmasked free thiol groups of cysteine residues. The biotin-conjugated proteins were then eluted with 2× SDS loading buffer, subjected to SDS-PAGE, and blotted with streptavidin-HRP antibody (Thermo Scientific) or mouse anti-FLAG antibody (catalog no. 8146, Cell Signaling Technology, Danvers, MA).

Statistical Analysis—Data were analyzed and plotted using SigmaPlot 12 (Systat Software) and expressed as means ± S.D., where S.D. is standard deviation. One-way analysis of variance with a post-hoc test (Bonferroni adjustment) was used to compare two sets of data. A probability value (p) of less than 0.05, 0.01, and 0.001 was considered statistically significant and indicated by *, **, and ***, respectively.

Author Contributions—W. Z., V. F., J. T., L. G. B., and X. Z. C. conceived and designed the experiment. W. Z., J. Y., E. B., R. C., S. H., L. H., and Q. L. performed the experiments. W. Z., V. F., J. T., L. G. B., and X. Z. C. analyzed the data. W. Z., J. F., and X. Z. C. wrote the paper.

References

1. Clapham, D. E. (2003) TRP channels as cellular sensors. *Nature* **426,** 517–524
2. Venkatachalam, K., and Montell, C. (2007) TRP channels. *Annu. Rev. Biochem.* **76,** 387–417

3. Liao, M., Cao, E., Julius, D., and Cheng, Y. (2013) Structure of the TRPV1 ion channel determined by electron cryo-microscopy. *Nature* **504,** 107–112
4. Paulsen, C. E., Armache, J. P., Gao, Y., Cheng, Y., and Julius, D. (2015) Structure of the TRPA1 ion channel suggests regulatory mechanisms. *Nature* **520,** 511–517
5. Zubcevic, L., Herzik, M. A., Jr, Chung, B. C., Liu, Z., Lander, G. C., and Lee, S. Y. (2016) Cryo-electron microscopy structure of the TRPV2 ion channel. *Nat. Struct. Mol. Biol.* **23,** 180–186
6. Saotome, K., Singh, A. K., Yelshanskaya, M. V., and Sobolevsky, A. I. (2016) Crystal structure of the epithelial calcium channel TRPV6. *Nature* **534,** 506–511
7. Mochizuki, T., Wu, G., Hayashi, T., Xenophontos, S. L., Veldhuisen, B., Saris, J. J., Reynolds, D. M., Cai, Y., Gabow, P. A., Pierides, A., Kimberling, W. J., Breuning, M. H., Deltas, C. C., Peters, D. J., and Somlo, S. (1996) PKD2, a gene for polycystic kidney disease that encodes an integral membrane protein. *Science* **272,** 1339–1342
8. Huang, A. L., Chen, X., Hoon, M. A., Chandrashekar, J., Guo, W., Tränkner, D., Ryba, N. J., and Zuker, C. S. (2006) The cells and logic for mammalian sour taste detection. *Nature* **442,** 934–938
9. Ishimaru, Y., Inada, H., Kubota, M., Zhuang, H., Tominaga, M., and Matsunami, H. (2006) Transient receptor potential family members PKD1L3 and PKD2L1 form a candidate sour taste receptor. *Proc. Natl. Acad. Sci. U.S.A.* **103,** 12569–12574
10. LopezJimenez, N. D., Cavenagh, M. M., Sainz, E., Cruz-Ithier, M. A., Battey, J. F., and Sullivan, S. L. (2006) Two members of the TRPP family of ion channels, Pkd1l3 and Pkd2l1, are co-expressed in a subset of taste receptor cells. *J. Neurochem.* **98,** 68–77
11. Horio, N., Yoshida, R., Yasumatsu, K., Yanagawa, Y., Ishimaru, Y., Matsunami, H., and Ninomiya, Y. (2011) Sour taste responses in mice lacking PKD channels. *PLoS One* **6,** e20007
12. Djenoune, L., Khabou, H., Joubert, F., Quan, F. B., Nunes Figueiredo, S., Bodineau, L., Del Bene, F., Burcklé, C., Tostivint, H., and Wyart, C. (2014) Investigation of spinal cerebrospinal fluid-contacting neurons expressing PKD2L1: evidence for a conserved system from fish to primates. *Front. Neuroanat.* **8,** 26
13. Orts-Del'Immagine, A., Kastner, A., Tillement, V., Tardivel, C., Trouslard, J., and Wanaverbecq, N. (2014) Morphology, distribution and phenotype of polycystin kidney disease 2-like 1-positive cerebrospinal fluid contacting neurons in the brainstem of adult mice. *PLoS One* **9,** e87748
14. Nomura, H., Turco, A. E., Pei, Y., Kalaydjieva, L., Schiavello, T., Weremowicz, S., Ji, W., Morton, C. C., Meisler, M., Reeders, S. T., and Zhou, J. (1998) Identification of PKDL, a novel polycystic kidney disease 2-like gene whose murine homologue is deleted in mice with kidney and retinal defects. *J. Biol. Chem.* **273,** 25967–25973
15. Chen, X. Z., Vassilev, P. M., Basora, N., Peng, J. B., Nomura, H., Segal, Y., Brown, E. M., Reeders, S. T., Hediger, M. A., and Zhou, J. (1999) Polycystin-L is a calcium-regulated cation channel permeable to calcium ions. *Nature* **401,** 383–386
16. Zheng, W., Hussein, S., Yang, J., Huang, J., Zhang, F., Hernandez-Anzaldo, S., Fernandez-Patron, C., Cao, Y., Zeng, H., Tang, J., and Chen, X. Z. (2015) A novel PKD2L1 C-terminal domain critical for trimerization and channel function. *Sci. Rep.* **5,** 9460
17. Li, Q., Dai, X. Q., Shen, P. Y., Wu, Y., Long, W., Chen, C. X., Hussain, Z., Wang, S., and Chen, X. Z. (2007) Direct binding of α-actinin enhances TRPP3 channel activity. *J. Neurochem.* **103,** 2391–2400
18. Murakami, M., Ohba, T., Xu, F., Shida, S., Satoh, E., Ono, K., Miyoshi, I., Watanabe, H., Ito, H., and Iijima, T. (2005) Genomic organization and functional analysis of murine PKD2L1. *J. Biol. Chem.* **280,** 5626–5635
19. Inada, H., Kawabata, F., Ishimaru, Y., Fushiki, T., Matsunami, H., and Tominaga, M. (2008) Off-response property of an acid-activated cation channel complex PKD1L3-PKD2L1. *EMBO Rep.* **9,** 690–697
20. DeCaen, P. G., Delling, M., Vien, T. N., and Clapham, D. E. (2013) Direct recording and molecular identification of the calcium channel of primary cilia. *Nature* **504,** 315–318
21. Delling, M., DeCaen, P. G., Doerner, J. F., Febvay, S., and Clapham, D. E. (2013) Primary cilia are specialized calcium signalling organelles. *Nature* **504,** 311–314
22. Cai, Y., Anyatonwu, G., Okuhara, D., Lee, K. B., Yu, Z., Onoe, T., Mei, C. L., Qian, Q., Geng, L., Wiztgall, R., Ehrlich, B. E., and Somlo, S. (2004) Calcium dependence of polycystin-2 channel activity is modulated by phosphorylation at Ser812. *J. Biol. Chem.* **279,** 19987–19995
23. Streets, A. J., Moon, D. J., Kane, M. E., Obara, T., and Ong, A. C. (2006) Identification of an N-terminal glycogen synthase kinase 3 phosphorylation site which regulates the functional localization of polycystin-2 *in vivo* and *in vitro*. *Hum. Mol. Genet.* **15,** 1465–1473
24. Cai, Y., Maeda, Y., Cedzich, A., Torres, V. E., Wu, G., Hayashi, T., Mochizuki, T., Park, J. H., Witzgall, R., and Somlo, S. (1999) Identification and characterization of polycystin-2, the PKD2 gene product. *J. Biol. Chem.* **274,** 28557–28565
25. Yeste-Velasco, M., Linder, M. E., and Lu, Y. J. (2015) Protein *S*-palmitoylation and cancer. *Biochim. Biophys. Acta* **1856,** 107–120
26. Tsutsumi, R., Fukata, Y., and Fukata, M. (2008) Discovery of protein-palmitoylating enzymes. *Pflugers Arch.* **456,** 1199–1206
27. Fernández-Hernando, C., Fukata, M., Bernatchez, P. N., Fukata, Y., Lin, M. I., Bredt, D. S., and Sessa, W. C. (2006) Identification of Golgi-localized acyl transferases that palmitoylate and regulate endothelial nitric oxide synthase. *J. Cell Biol.* **174,** 369–377
28. Moffett, S., Rousseau, G., Lagacé, M., and Bouvier, M. (2001) The palmitoylation state of the β(2)-adrenergic receptor regulates the synergistic action of cyclic AMP-dependent protein kinase and β-adrenergic receptor kinase involved in its phosphorylation and desensitization. *J. Neurochem.* **76,** 269–279
29. Loisel, T. P., Ansanay, H., Adam, L., Marullo, S., Seifert, R., Lagacé, M., and Bouvier, M. (1999) Activation of the β_2-adrenergic receptor-Gγ(s) complex leads to rapid depalmitoylation and inhibition of repalmitoylation of both the receptor and Gα(s). *J. Biol. Chem.* **274,** 31014–31019
30. Moffett, S., Adam, L., Bonin, H., Loisel, T. P., Bouvier, M., and Mouillac, B. (1996) Palmitoylated cysteine 341 modulates phosphorylation of the β2-adrenergic receptor by the cAMP-dependent protein kinase. *J. Biol. Chem.* **271,** 21490–21497
31. Shipston, M. J. (2014) Ion channel regulation by protein *S*-acylation. *J. Gen. Physiol.* **143,** 659–678
32. Vergarajauregui, S., and Puertollano, R. (2006) Two di-leucine motifs regulate trafficking of mucolipin-1 to lysosomes. *Traffic* **7,** 337–353
33. Chandra, M., Zhou, H., Li, Q., Muallem, S., Hofmann, S. L., and Soyombo, A. A. (2011) A role for the Ca^{2+} channel TRPML1 in gastric acid secretion, based on analysis of knockout mice. *Gastroenterology* **140,** 857–867
34. Ishimaru, Y., Katano, Y., Yamamoto, K., Akiba, M., Misaka, T., Roberts, R. W., Asakura, T., Matsunami, H., and Abe, K. (2010) Interaction between PKD1L3 and PKD2L1 through their transmembrane domains is required for localization of PKD2L1 at taste pores in taste cells of circumvallate and foliate papillae. *FASEB J.* **24,** 4058–4067
35. Feng, S., Rodat-Despoix, L., Delmas, P., and Ong, A. C. (2011) A single amino acid residue constitutes the third dimerization domain essential for the assembly and function of the tetrameric polycystin-2 (TRPP2) channel. *J. Biol. Chem.* **286,** 18994–19000
36. Bosmans, F., Milescu, M., and Swartz, K. J. (2011) Palmitoylation influences the function and pharmacology of sodium channels. *Proc. Natl. Acad. Sci. U.S.A.* **108,** 20213–20218
37. Blaskovic, S., Blanc, M., and van der Goot, F. G. (2013) What does *S*-palmitoylation do to membrane proteins? *FEBS J.* **280,** 2766–2774
38. Lin, D. T., and Conibear, E. (2015) ABHD17 proteins are novel protein depalmitoylases that regulate N-Ras palmitate turnover and subcellular localization. *Elife* **4,** e11306
39. Tian, L., Jeffries, O., McClafferty, H., Molyvdas, A., Rowe, I. C., Saleem, F., Chen, L., Greaves, J., Chamberlain, L. H., Knaus, H. G., Ruth, P., and Shipston, M. J. (2008) Palmitoylation gates phosphorylation-dependent regulation of BK potassium channels. *Proc. Natl. Acad. Sci. U.S.A.* **105,** 21006–21011
40. Moritz, A. E., Rastedt, D. E., Stanislowski, D. J., Shetty, M., Smith, M. A., Vaughan, R. A., and Foster, J. D. (2015) Reciprocal phosphorylation and palmitoylation control dopamine transporter kinetics. *J. Biol. Chem.* **290,** 29095–29105
41. Yang, J., Wang, Q., Zheng, W., Tuli, J., Li, Q., Wu, Y., Hussein, S., Dai, X. Q., Shafiei, S., Li, X. G., Shen, P. Y., Tu, J. C., and Chen, X. Z. (2012)

Receptor for activated C kinase 1 (RACK1) inhibits function of transient receptor potential (TRP)-type channel Pkd2L1 through physical interaction. *J. Biol. Chem.* **287,** 6551–6561

42. Gauthier-Kemper, A., Igaev, M., Sündermann, F., Janning, D., Brühmann, J., Moschner, K., Reyher, H. J., Junge, W., Glebov, K., Walter, J., Bakota, L., and Brandt, R. (2014) Interplay between phosphorylation and palmitoylation mediates plasma membrane targeting and sorting of GAP43. *Mol. Biol. Cell* **25,** 3284–3299
43. Schmidt, M. F., and Schlesinger, M. J. (1979) Fatty acid binding to vesicular stomatitis virus glycoprotein: a new type of post-translational modification of the viral glycoprotein. *Cell* **17,** 813–819
44. Schmidt, J. W., and Catterall, W. A. (1987) Palmitylation, sulfation, and glycosylation of the α subunit of the sodium channel. Role of post-translational modifications in channel assembly. *J. Biol. Chem.* **262,** 13713–13723
45. Liu, C., and Montell, C. (2015) Forcing open TRP channels: mechanical gating as a unifying activation mechanism. *Biochem. Biophys. Res. Commun.* **460,** 22–25
46. Nauli, S. M., Alenghat, F. J., Luo, Y., Williams, E., Vassilev, P., Li, X., Elia, A. E., Lu, W., Brown, E. M., Quinn, S. J., Ingber, D. E., and Zhou, J. (2003) Polycystins 1 and 2 mediate mechanosensation in the primary cilium of kidney cells. *Nat. Genet.* **33,** 129–137
47. Yao, G., Luo, C., Harvey, M., Wu, M., Schreiber, T. H., Du, Y., Basora, N., Su, X., Contreras, D., and Zhou, J. (2016) Disruption of polycystin-L causes hippocampal and thalamocortical hyperexcitability. *Hum. Mol. Genet.* **25,** 448–458
48. el-Husseini Ael-D, and Bredt, D. S. (2002) Protein palmitoylation: a regulator of neuronal development and function. *Nat. Rev. Neurosci.* **3,** 791–802
49. Wedegaertner, P. B., and Bourne, H. R. (1994) Activation and depalmitoylation of Gsα. *Cell* **77,** 1063–1070
50. Voolstra, O., and Huber, A. (2014) Post-translational modifications of TRP channels. *Cells* **3,** 258–287
51. Li, Q., Liu, Y., Zhao, W., and Chen, X. Z. (2002) The calcium-binding EF-hand in polycystin-L is not a domain for channel activation and ensuing inactivation. *FEBS Lett.* **516,** 270–278
52. Brigidi, G. S., and Bamji, S. X. (2013) Detection of protein palmitoylation in cultured hippocampal neurons by immunoprecipitation and acyl-biotin exchange (ABE). *J. Vis. Exp.* 2013 50031
53. Hussein, S., Zheng, W., Dyte, C., Wang, Q., Yang, J., Zhang, F., Tang, J., Cao, Y., and Chen, X. Z. (2015) Acid-induced off-response of PKD2L1 channel in Xenopus oocytes and roles of Ca^{2+}. *Sci. Rep.* **5,** 15752